

# Supporting Information for:

## A quasilinear hydrazone-based mononuclear dysprosium compound in weak easy-plane anisotropy exhibiting field-induced complex magnetic relaxation<sup>†</sup>

Peiqiong Chen,<sup>‡a</sup> Xiao Sun,<sup>‡a</sup> Xuefeng Guo,<sup>b</sup> Dan Liu,<sup>\*b</sup> Hou-Ting Liu,<sup>a</sup> Jing Lu<sup>\*a</sup> and Haiquan Tian<sup>\*a</sup>

<sup>a</sup> Shandong Provincial Key Laboratory of Chemical Energy Storage and Novel Cell Technology, School of Chemistry and Chemical Engineering, Liaocheng University, Liaocheng 252059, P. R. China. E-mail: [tianhaiquan@lcu.edu.cn](mailto:tianhaiquan@lcu.edu.cn), [lujing@lcu.edu.cn](mailto:lujing@lcu.edu.cn)

<sup>b</sup> Institute of Flexible Electronics, Northwestern Polytechnical University, 127 West Youyi Road, Xi'an, 710072, Shaanxi, China. E-mail: [iamdliu@nwpu.edu.cn](mailto:iamdliu@nwpu.edu.cn)

<sup>‡</sup> These authors contributed equally to this work.

**Table S1.** Selected bond lengths ( $\text{\AA}$ ) and angles ( $^\circ$ ) for compound **I**.

Compound I					
Dy1–O1	2.432(7)	O1-Dy1-N12	71.0(2)	N5-Dy1-N9	131.2(2)
Dy1–O2	2.493(7)	O1-Dy1-N13	135.9(3)	N5-Dy1-N10	149.0(2)
Dy1–N4	2.519(7)	O2-Dy1-N4	67.7(2)	N5-Dy1-N11	74.3(3)
Dy1–N5	2.584(7)	O2-Dy1-N5	76.7(2)	N5-Dy1-N12	103.3(2)
Dy1–N9	2.510(6)	O2-Dy1-N9	62.9(2)	N5-Dy1-N13	76.4(3)
Dy1–N10	2.605(7)	O2-Dy1-N10	125.2(2)	N9-Dy1-N10	62.4(2)
Dy1–N11	2.408(9)	O2-Dy1-N11	142.6(3)	N9-Dy1-N11	124.2(3)
Dy1–N12	2.411(7)	O2-Dy1-N12	135.7(2)	N9-Dy1-N12	68.4(3)
Dy1–N13	2.399(8)	O2-Dy1-N13	75.9(3)	N9-Dy1-N13	68.4(3)
O1-Dy1-O2	73.2(2)	N4-Dy1-N5	62.2(2)	N10-Dy1-N11	76.0(3)
O1-Dy1-N4	63.5(2)	N4-Dy1-N9	119.1(2)	N10-Dy1-N12	76.7(2)
O1-Dy1-N5	124.6(2)	N4-Dy1-N10	142.2(2)	N10-Dy1-N13	87.7(3)
O1-Dy1-N9	69.8(2)	N4-Dy1-N11	116.6(3)	N11-Dy1-N12	74.6(3)
O1-Dy1-N10	85.3(2)	N4-Dy1-N12	73.4(2)	N11-Dy1-N13	74.7(3)
O1-Dy1-N11	143.8(3)	N4-Dy1-N13	129.4(3)	N12-Dy1-N13	148.1(3)

Symmetry codes: (a) 1.5-x, 1-y, z.

**Table S2.** Hydrogen bonds in compound I.

Compound I				
D-H···A	d(D-H) (Å)	d(H···A) (Å)	d(D···A) (Å)	∠(DHA) (°)
N3-H3A···O3	0.8800	1.9000	2.739(11)	158.00
C2-H2···N8	0.9500	2.0500	2.934(11)	154.00
C4-H4···O3	0.9500	2.3300	3.273(13)	172.00
C4-H4···N3	0.9500	2.3300	2.680(11)	101.00
C11-H11···N13	0.9500	2.5800	3.117(13)	116.00
C15-H15···N8	0.9500	2.3100	2.662(11)	101.00
C20-H20···S3	0.9500	2.7500	3.582(11)	146.00

Symmetry codes: (a) 1.5-x, 1-y, z; (b) 1.5-x, 1-y, z; (c) 1.5-x, 1-y, z; (d) 1.5-x, 0.5+y, 0.5-z.

**Table S3.** Dy<sup>III</sup> geometry analysis of **I** by SHAPE 2.1 software.

Compound I			
Geometry (CN = 9)	Dy1	Geometry (CN = 9)	Dy1
<b>EP-9</b>	35.886	<b>CSAPR-9</b>	0.822
<b>OPY-9</b>	22.710	<b>JTCTPR-9</b>	2.886
<b>HBPY-9</b>	19.947	<b>TCTPR-9</b>	1.474
<b>JTC-9</b>	15.761	<b>JTDIC-9</b>	12.137
<b>JCCU-9</b>	11.316	<b>HH-9</b>	10.599
<b>CCU-9</b>	9.379	<b>MFF-9</b>	1.471
<b>JCSAPR-9</b>	1.650		

Label	Shape	Label	Shape
<b>EP-9</b>	Enneagon ( $D_{9h}$ )	<b>CSAPR-9</b>	Spherical capped square antiprism ( $C_{4v}$ )
<b>OPY-9</b>	Octagonal pyramid ( $C_{8v}$ )	<b>JTCTPR-9</b>	Tricapped trigonal prism J51 ( $D_{3h}$ )
<b>HBPY-9</b>	Heptagonal bipyramid ( $D_{7h}$ )	<b>TCTPR-9</b>	Spherical tricapped trigonal prism ( $D_{3h}$ )
<b>JTC-9</b>	Johnson triangular cupola J3 ( $C_{3v}$ )	<b>JTDIC-9</b>	Tridiminished icosahedron J63 ( $C_{3v}$ )
<b>JCCU-9</b>	Capped cube J8 ( $C_{4v}$ )	<b>HH-9</b>	Hula-hoop ( $C_{2v}$ )
<b>CCU-9</b>	Spherical-relaxed capped cube ( $C_{4v}$ )	<b>MFF-9</b>	Muffin ( $C_s$ )
<b>JCSAPR-9</b>	Capped square antiprism J10 ( $C_{4v}$ )		

**Table S4.** Relaxation fitting parameters from least-squares fitting of  $\chi(\omega)$  data for compound I.

<b>T</b>	$\chi_{s, \text{tot}}$	<b>FR</b>			<b>SR</b>		
		$\Delta\chi_1$	$\alpha_1$	$\ln(\tau_1 / \text{s})$	$\Delta\chi_2$	$\alpha_2$	$\ln(\tau_2 / \text{s})$
1.9	-8.457(9)	33.86(1)	0.191(4)	-1.598(2)	0.65(1)	0.293(5)	-7.401(3)
2.2	-10.329(7)	28.97(5)	0.176(9)	-1.609(9)	4.32(8)	0.263(1)	-7.482(8)
2.5	-12.521(5)	21.15(9)	0.154(3)	-1.685(4)	10.81(5)	0.257(1)	-7.810(1)
3.0	-15.320(7)	15.46(3)	0.117(1)	-1.653(4)	14.07(1)	0.229(5)	-8.611(2)
3.5	-17.614(8)	10.51(9)	0.101(7)	-1.642(5)	18.90(7)	0.216(7)	-9.840(3)
4.0	-19.906(8)	8.643(1)	0.092(9)	--	20.68(5)	0.194(3)	-11.165(7)
4.5	-21.464(1)	6.837(5)	0.087(8)	--	22.08(1)	0.179(1)	-13.103(2)
5.0	-22.236(2)	4.959(8)	0.075(5)	--	23.75(9)	0.170(3)	-14.802(9)

**Table S5.** Relaxation fitting parameters from least-squares fitting of  $\chi(\omega)$  data under the dc applied field for I.

		FR			SR		
F (Oe)	$\chi_{s, \text{tot}}$	$\Delta\chi_1$	$\alpha_1$	$\tau_1 / \text{s}$	$\Delta\chi_2$	$\alpha_2$	$\tau_2 / \text{s}$
200	1.369(7)	0.057(1)	0.051(9)	0.1159(5)	0.620(8)	0.544(2)	8.038(3)E-4
400	0.669(7)	0.278(1)	0.077(4)	0.1195(9)	1.219(9)	0.455(8)	0.0012(1)
600	0.358(3)	0.216(5)	0.089(7)	0.1270(6)	1.377(2)	0.176(7)	0.0014(7)
800	0.194(2)	0.368(8)	0.093(9)	0.1354(9)	1.334(8)	0.175(7)	0.0014(8)
1000	0.077(4)	0.416(3)	0.103(4)	0.1461(2)	1.239(8)	0.093(6)	0.0013(5)
1200	-0.032(9)	0.618(3)	0.104(3)	0.1657(7)	1.094(8)	0.181(7)	0.0011(1)
1400	-0.293(2)	3.582(9)	0.086(3)	0.1799(9)	0.893(1)	0.500(8)	8.356(7)E-4
1600	-0.177(4)	2.160(1)	0.103(1)	0.1928(3)	0.802(7)	0.421(6)	6.296(2)E-4
1800	-0.160(2)	0.743(1)	0.163(2)	0.2146(6)	0.769(8)	0.192(4)	4.756(3)E-4
2000	-0.097(9)	0.674(4)	0.209(9)	0.2352(5)	0.712(7)	0.185(5)	3.360(3)E-4
2200	-0.009(9)	0.678(6)	0.252(6)	0.2460(7)	0.660(5)	0.138(8)	2.262(8)E-4
2400	0.076(8)	0.688(5)	0.281(3)	0.2642(2)	0.605(5)	0.164(3)	1.513(2)E-4
2600	0.147(5)	0.717(8)	0.330(9)	0.2845(9)	0.598(6)	0.193(6)	8.860(1)E-5
2800	0.042(6)	0.450(8)	0.532(5)	0.2936(5)	1.256(9)	0.051(8)	6.600(8)E-6
3000	0.156(6)	0.377(7)	0.560(6)	0.3032(7)	1.646(5)	0.031(4)	1.519(3)E-6

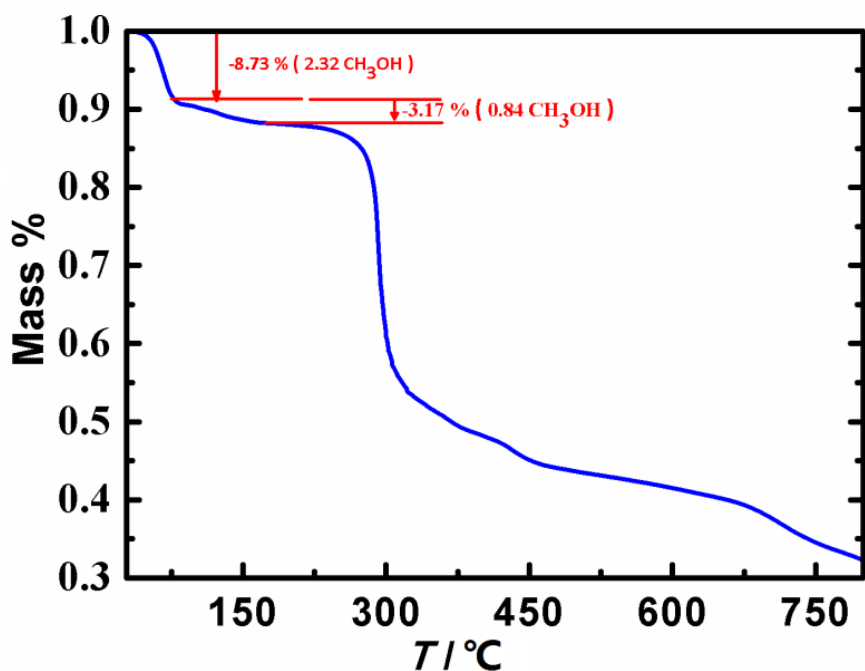


**Figure S1.** Thermal analysis of compound **I**.

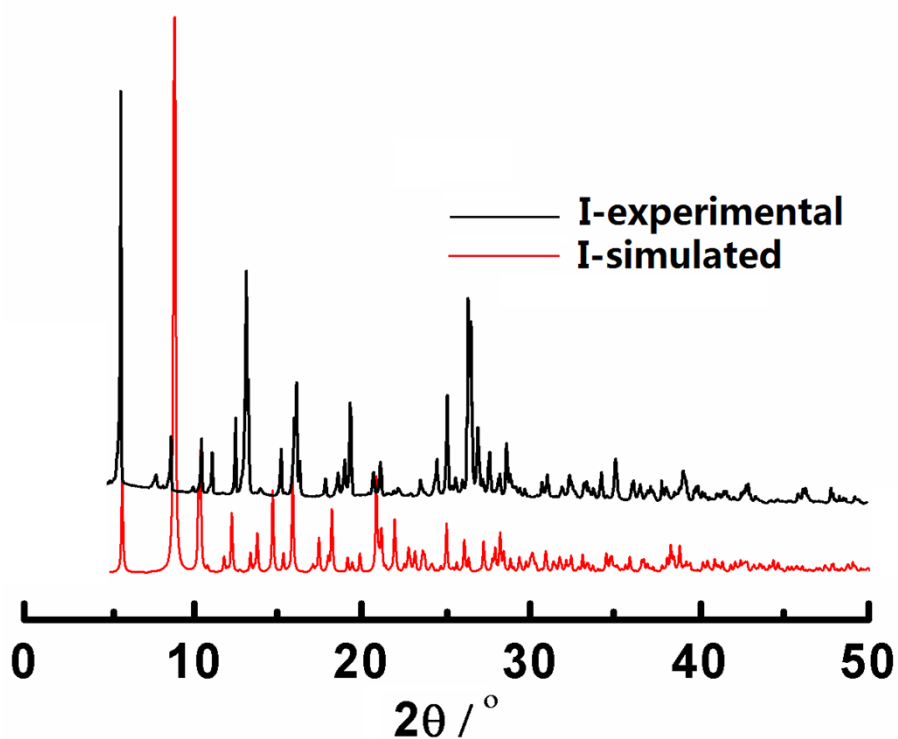


**Figure S2.** The powder XRD patterns for compound **I**.

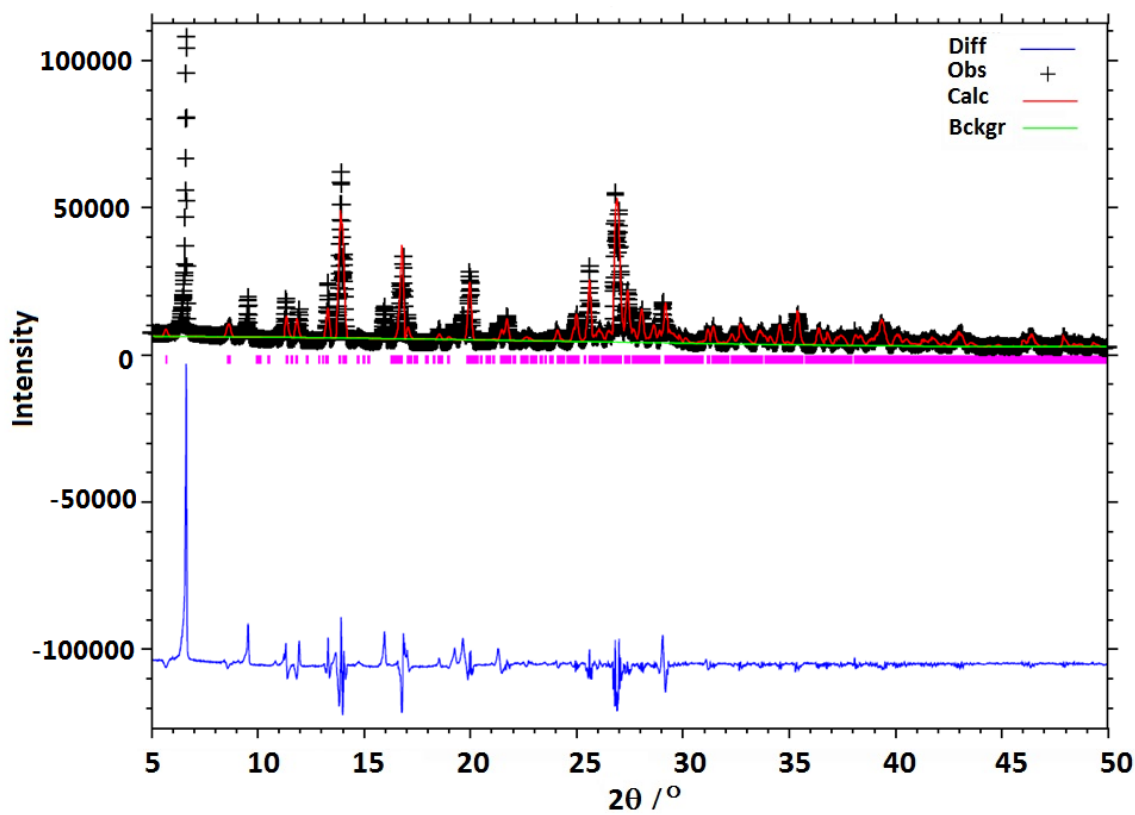


**Figure S3.** The black circles are for the observed data in **I**. The red solid line is for the calculated data. The grey solid curve is for the difference. The vertical bars are the positions of Bragg peaks. Cell parameters:  $Pbca$ ,  $a = 13.74 \text{ \AA}$ ,  $b = 17.50 \text{ \AA}$ ,  $c = 31.15 \text{ \AA}$ ,  $\alpha = 90.0^\circ$ ,  $\beta = 90.0^\circ$ ,  $\gamma = 90.0^\circ$ ,  $V = 7511.6 \text{ \AA}^3$  (wRp = 0.091). Thermal analysis of compound **I**.

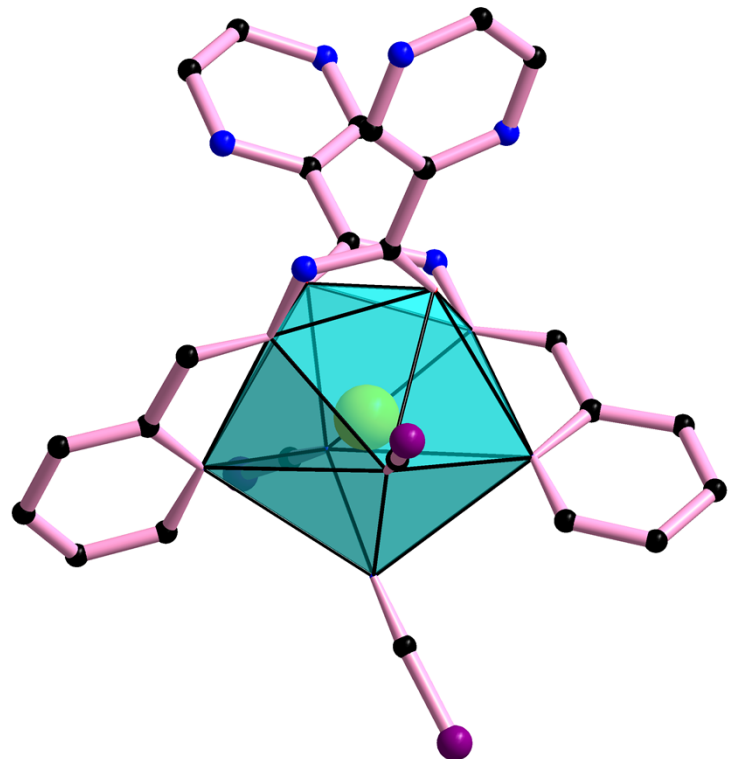


**Figure S4.** Coordination environments of the crystallographically independent  $\text{Dy}^{\text{III}}$  ion in **I**.

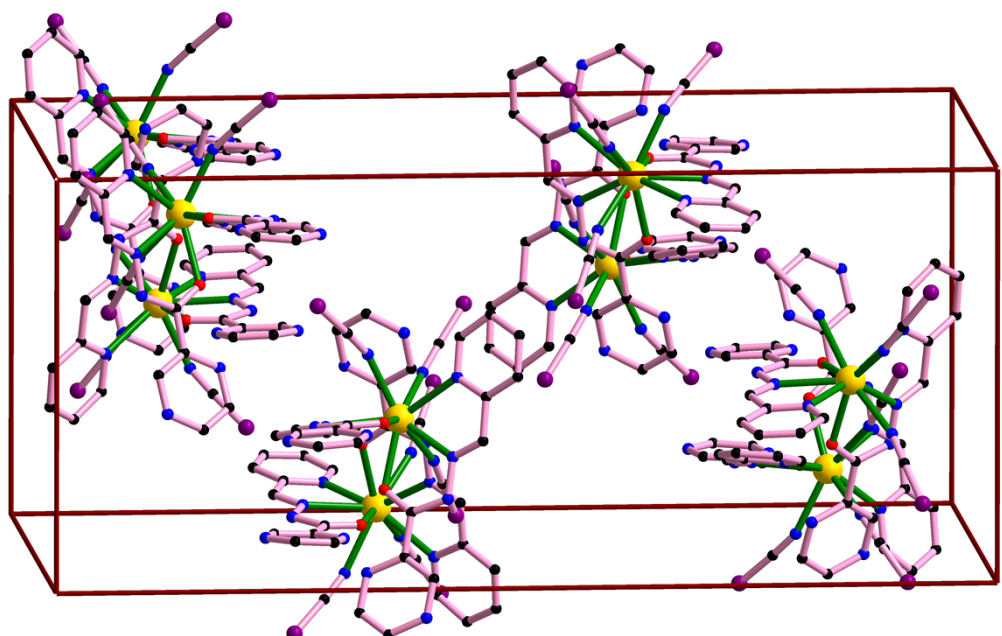


**Figure S5.** Unit cell of **I** showing the presence of eight crystallographically independent molecules.

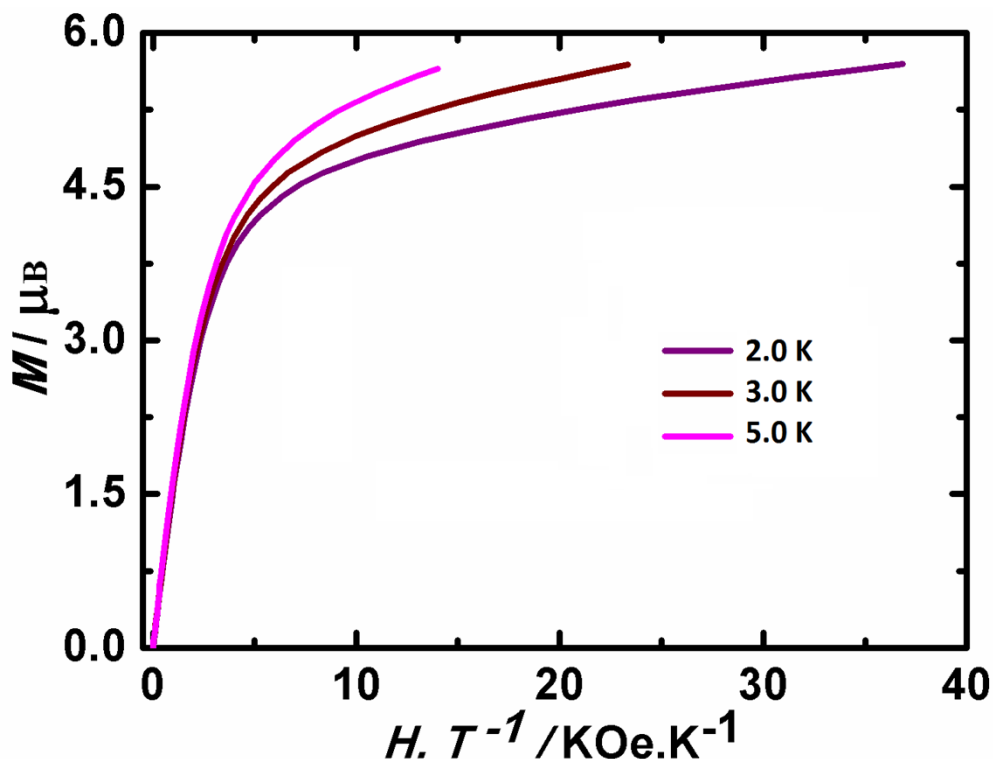


**Figure S6.** Magnetization data for compound **I** at temperature range of 2.0 K – 5.0 K.

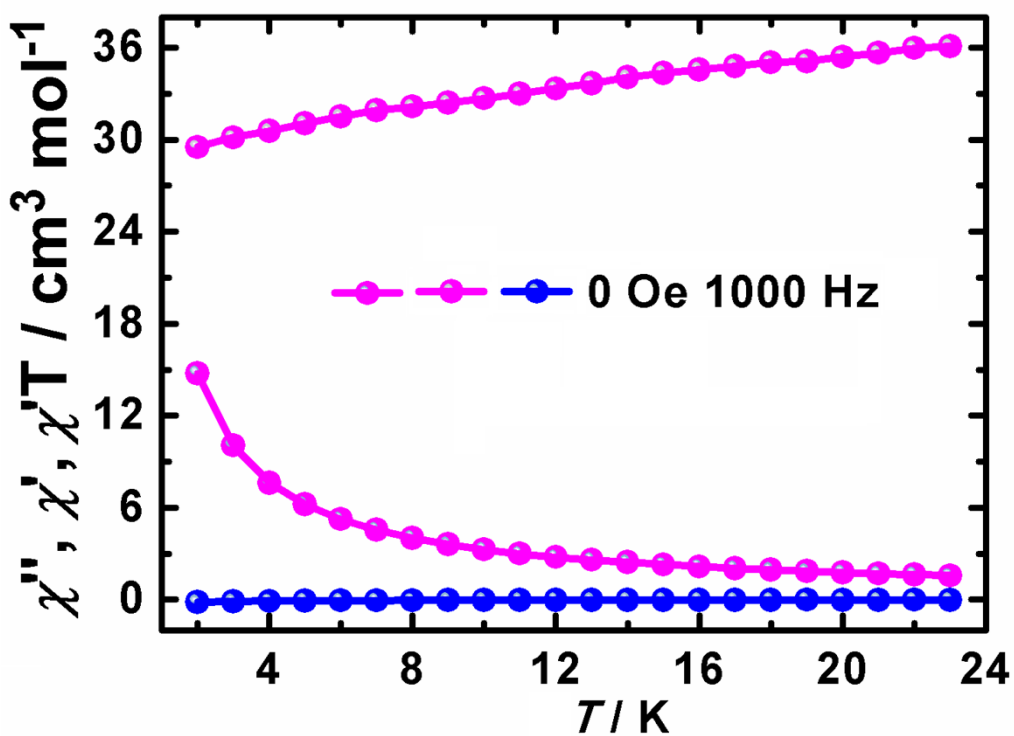


**Figure S7.** Temperature dependence of the  $\chi'T$ ,  $\chi'$  and  $\chi''$  ac susceptibilities under zero-dc field for compound **I**.

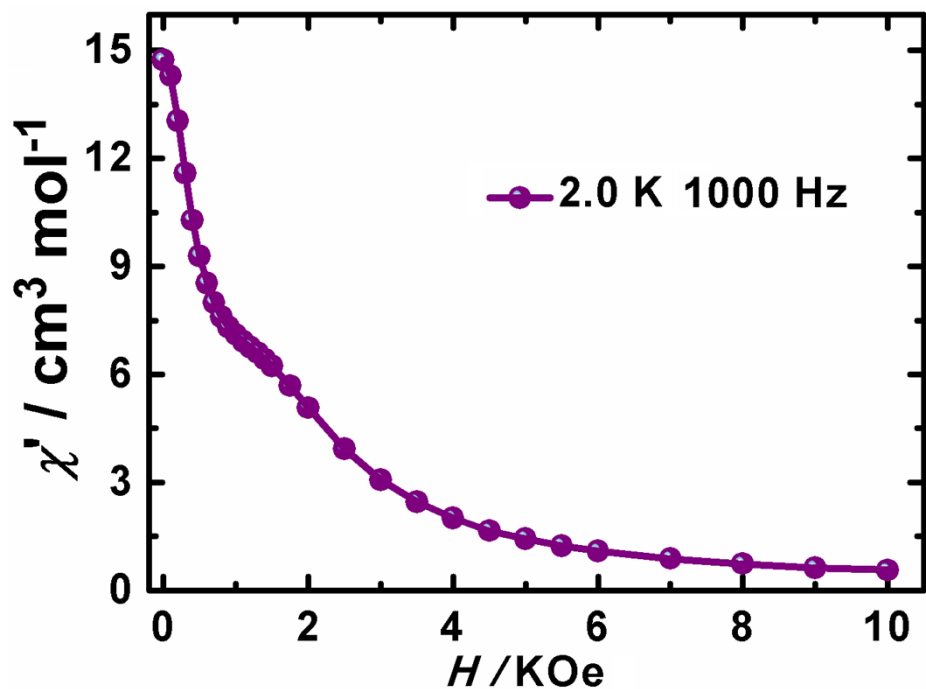


**Figure S8.** Field dependence of the  $\chi'$  ac susceptibility of compound I at 1000 Hz and 2 K.

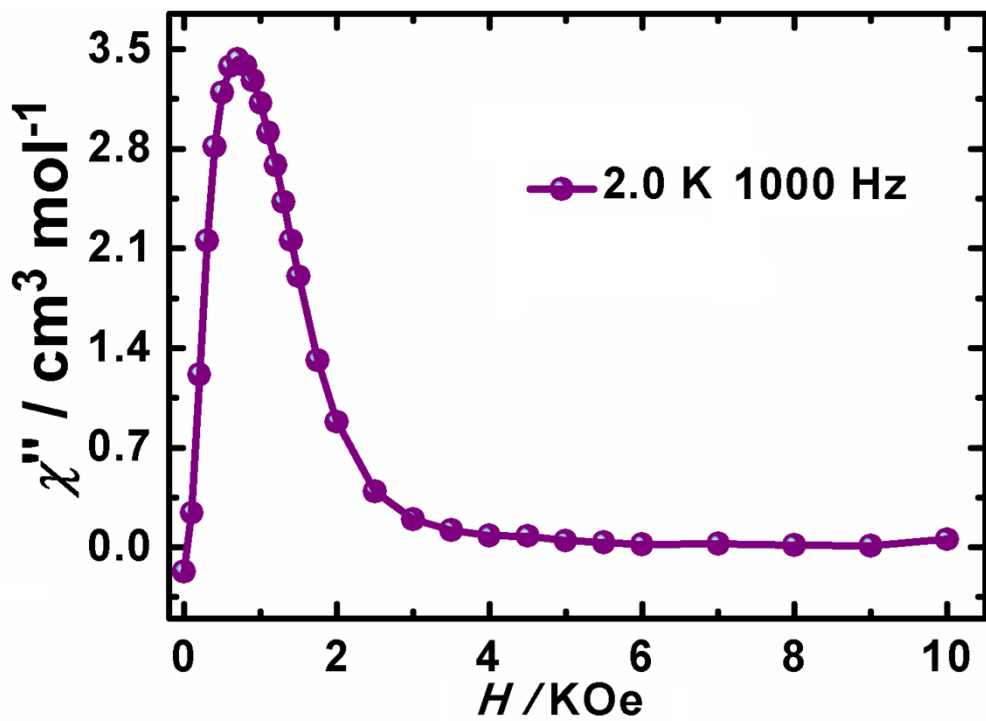


**Figure S9.** Field dependence of the  $\chi''$  ac susceptibility of compound I at 1000 Hz and 2 K.

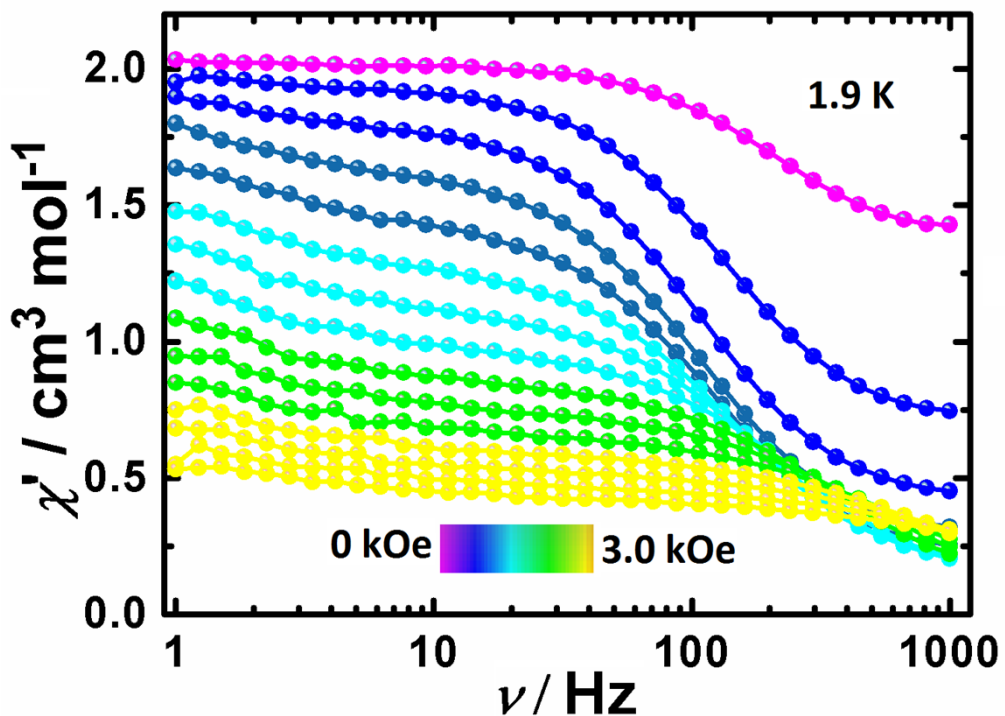


**Figure S10.** Frequency dependence of the  $\chi'$  ac susceptibility of compound I under various applied dc fields at 2.0 K.

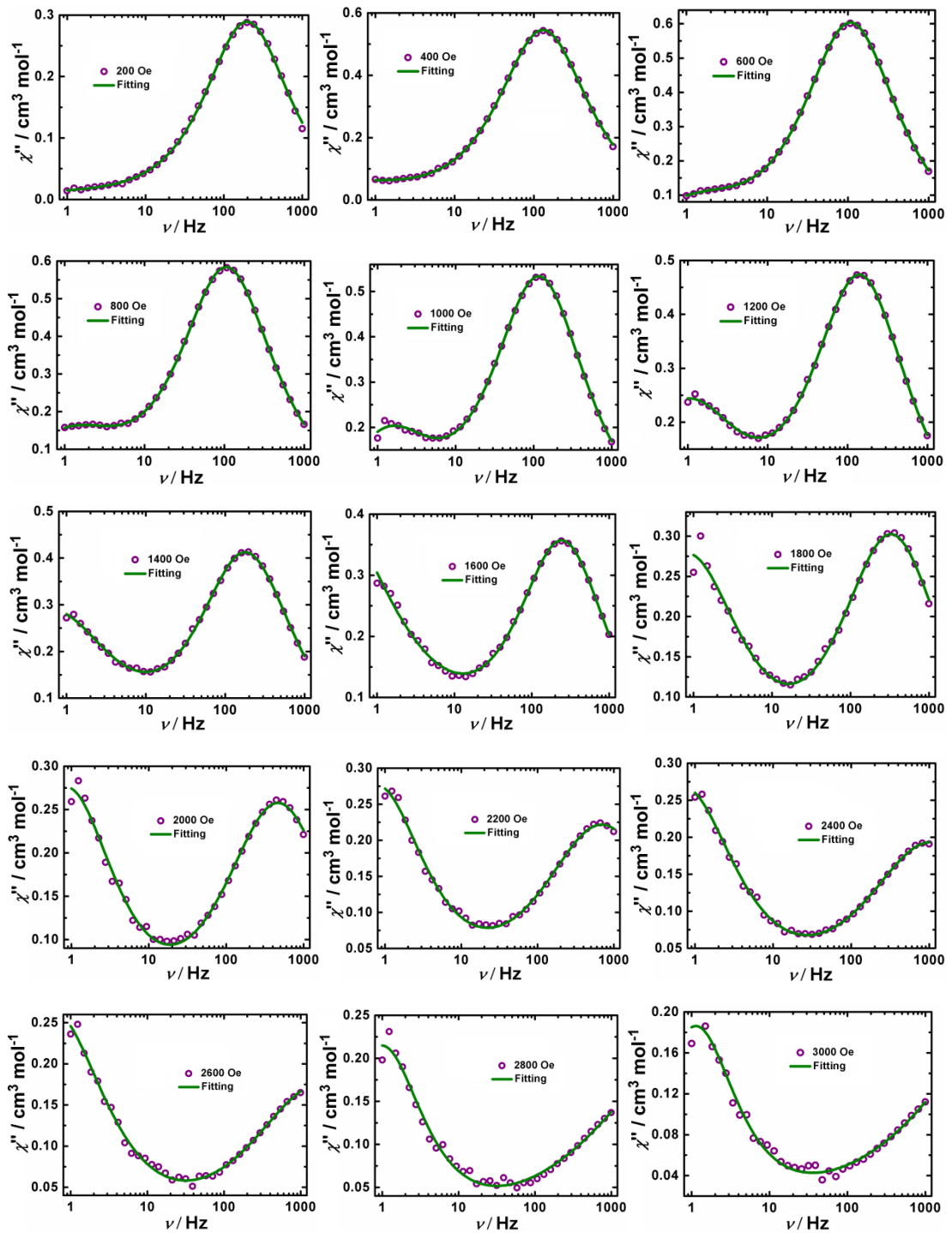


**Figure S11.** Frequency dependence of the out-of-phase ( $\chi''$ ) ac susceptibility of compound **I**. The solid lines represent the best fits.

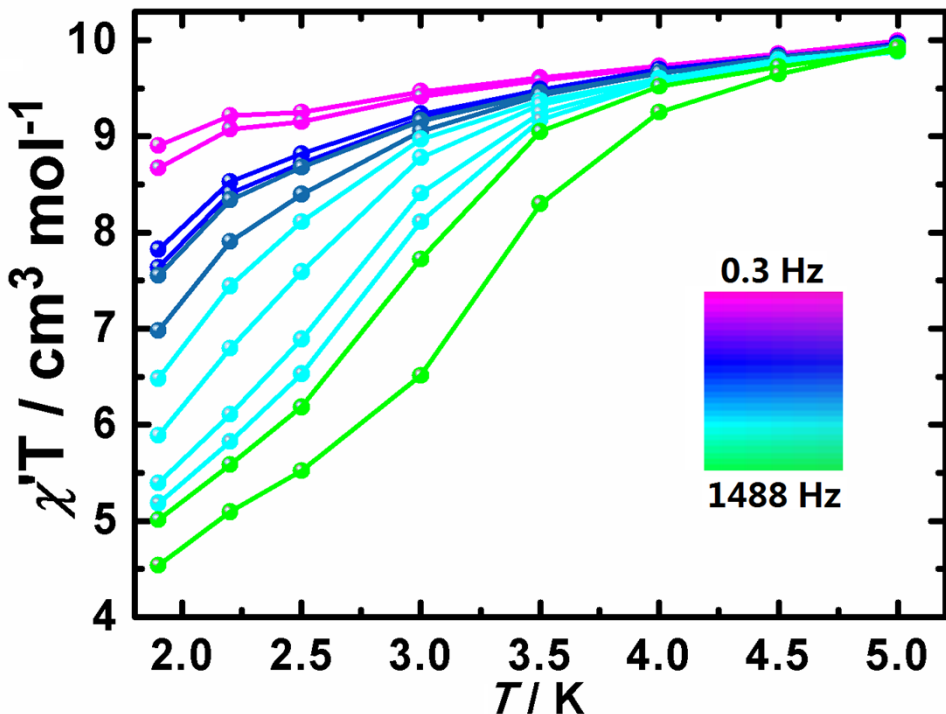


**Figure S12.** Temperature dependence of the  $\chi'T$  ac susceptibility under the optimal 0.7 kOe static field for I.

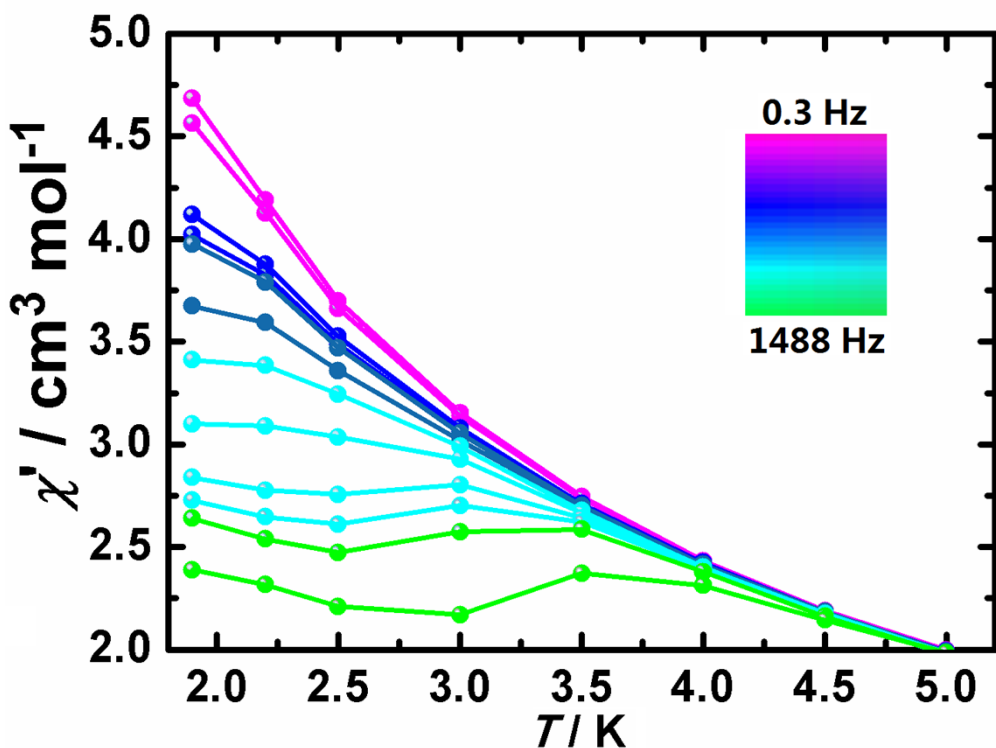


**Figure S13.** Temperature dependence of the  $\chi'$  product ac susceptibility under the optimal 0.7 kOe static field for I.

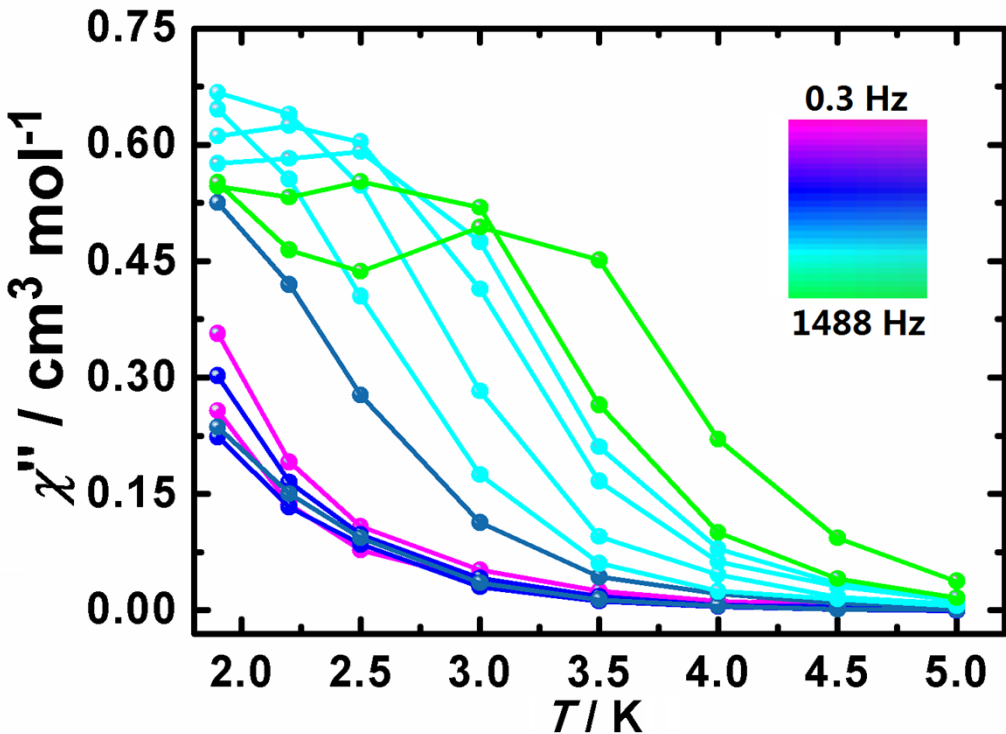


**Figure S14.** Temperature dependence of the  $\chi''$  product *ac* susceptibility under the optimal 0.7 kOe static field for **I**.

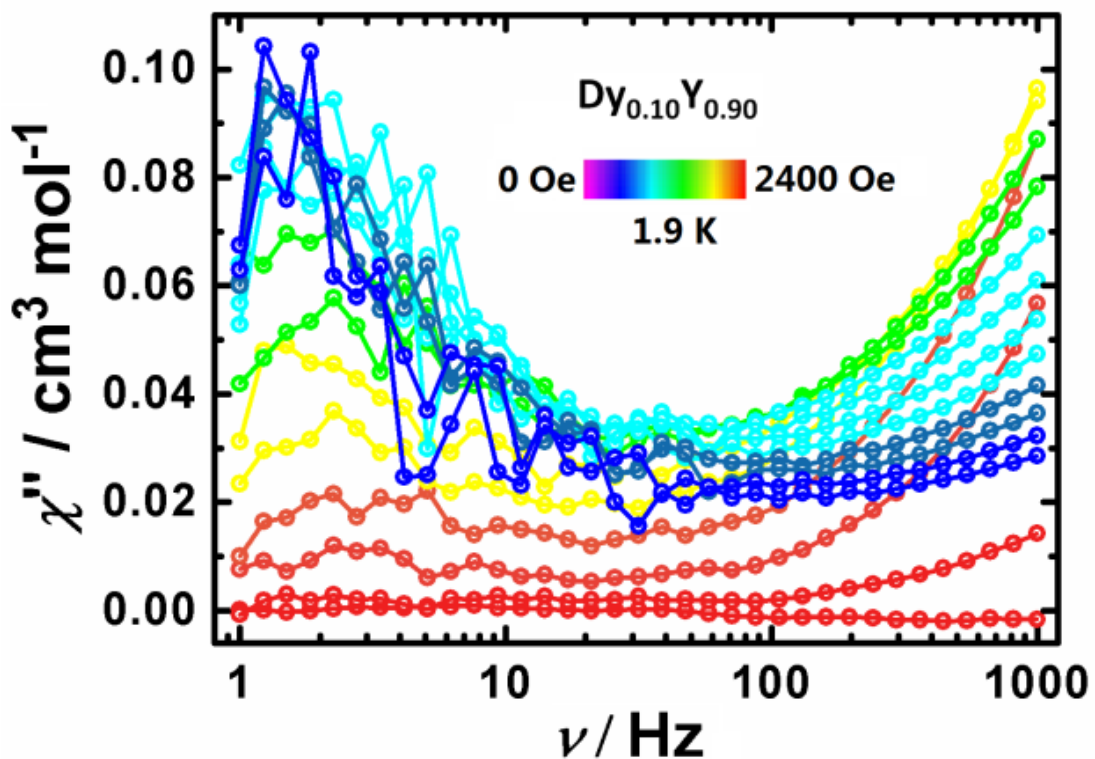


**Figure S15.** Variable-frequency out-of-phase ac susceptibility of  $\text{Dy}_{0.10}\text{Y}_{0.90}$  under various applied dc fields at 1.9 K.

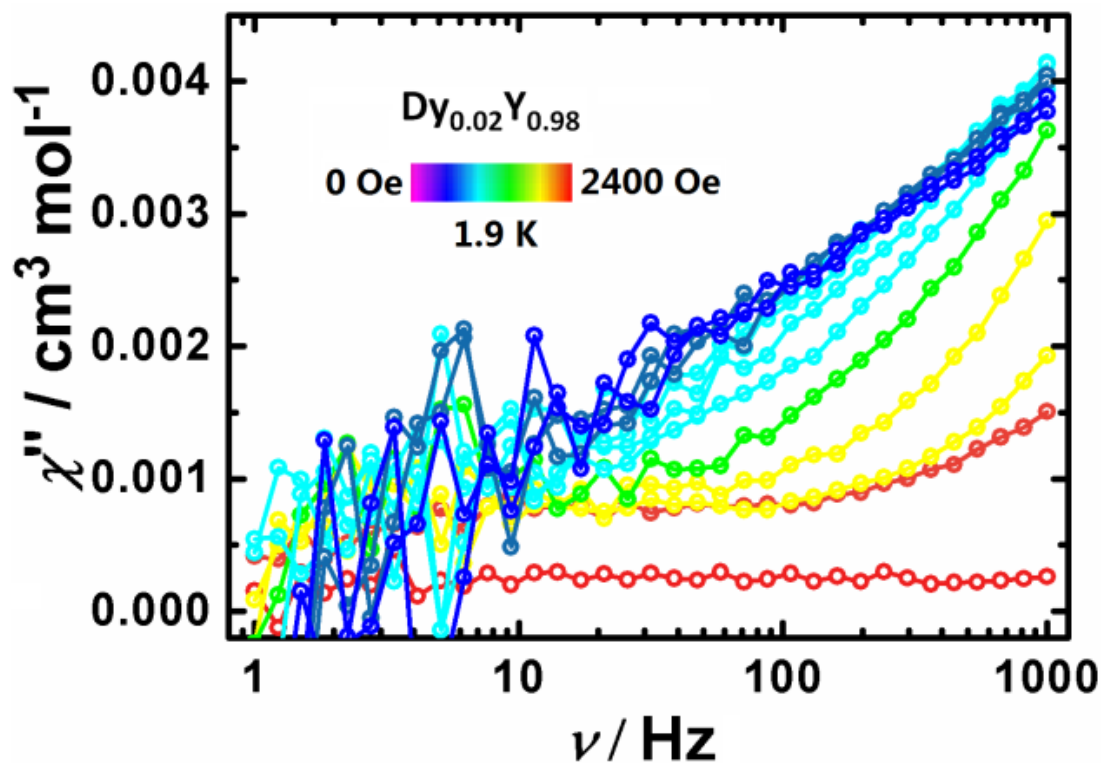


**Figure S16.** Variable-frequency out-of-phase ac susceptibility of  $\text{Dy}_{0.02}\text{Y}_{0.98}$  under various applied dc fields at 1.9 K.

## *Ab initio* calculations for Dy1 compound

All calculations were carried out with OpenMolcas<sup>S1</sup> and are of CASSCF/RASSI/SINGLE\_ANISO type.<sup>S2-S4</sup> Structure of Dy1 is shown in Figure1. Active space of the CASSCF method included 9 electrons in 7 orbitals for Dy (4f orbitals of Dy<sup>3+</sup> ion). On the basis of the resulting spin-orbital multiplets SINGLE\_ANISO program<sup>S5</sup> computed local magnetic properties (g-tensors, magnetic axes, local magnetic susceptibility etc.)

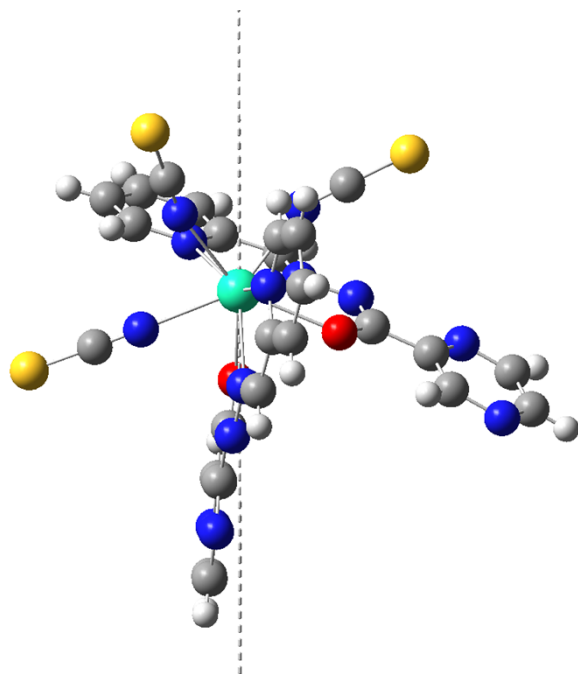


**Figure S17.** Structures of the Dy1 and main magnetic axis of ground doublet (dashed line).

**Table S6.** Contractions of the employed basis set in computational approximations for Dy1.

Basis set	
Dy	ANO-RCC-VTZP
N	ANO-RCC-VDZP
O	ANO-RCC-VDZ
C	ANO-RCC-VDZ
H	ANO-RCC-VDZ
S	ANO-RCC-VDZ

**Table S7.** Energies of the lowest Kramers doublets of Dy center in Dy1.

Spin-orbit energies (cm <sup>-1</sup> )	
	0.000
	31.291
	66.508
	104.337
	169.678
	230.905
	257.103
	321.977

**Table S8.** The g tensors of the lowest Kramers doublets (KD) of Dy center in Dy1.

KD		Dy in I
1	g <sub>x</sub>	0.648881335
	g <sub>y</sub>	2.113499404
	g <sub>z</sub>	17.656407339
2	g <sub>x</sub>	1.097740772
	g <sub>y</sub>	3.135091004
	g <sub>z</sub>	13.610809426
3	g <sub>x</sub>	2.694784315
	g <sub>y</sub>	5.356813725
	g <sub>z</sub>	10.348702742
4	g <sub>x</sub>	1.498748998
	g <sub>y</sub>	3.457086291
	g <sub>z</sub>	10.972704263

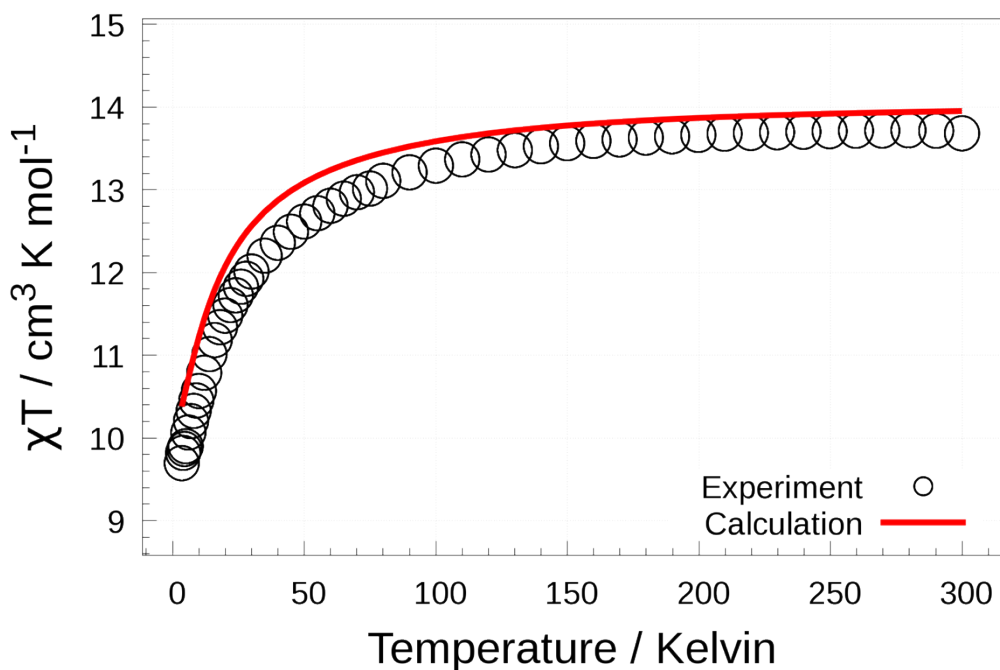


**Figure S18.** Experimental (circles) vs. calculated (red solid line) magnetic susceptibility of Dy1.

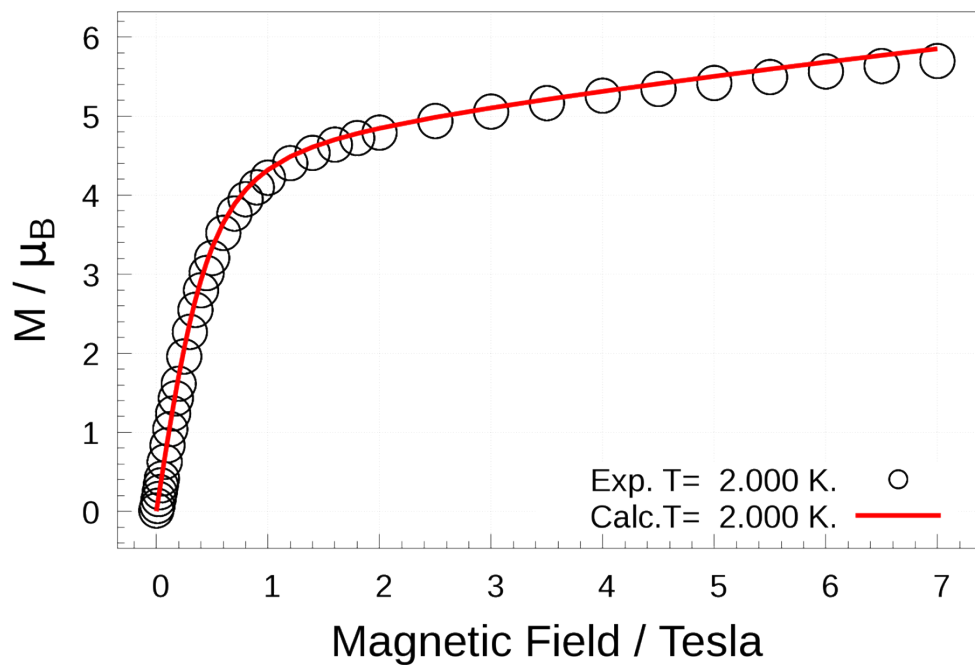


**Figure S19.** Experimental (circles) vs. calculated (red solid line) field-dependent magnetization of Dy1 at 2.0 K.

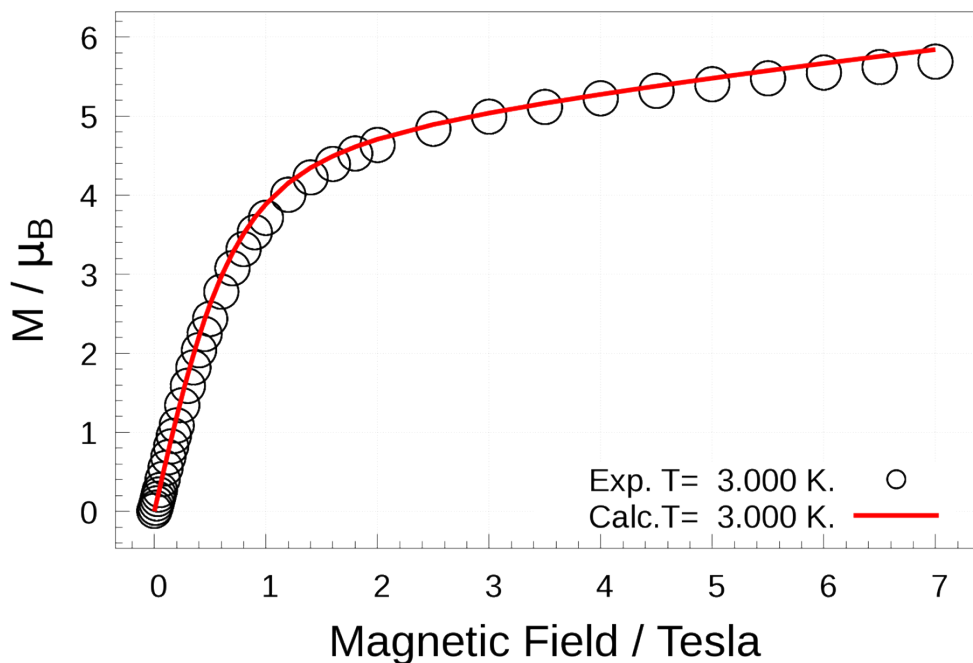


**Figure S20.** Experimental (circles) vs. calculated (red solid line) field-dependent magnetization of Dy1 at 3.0 K.

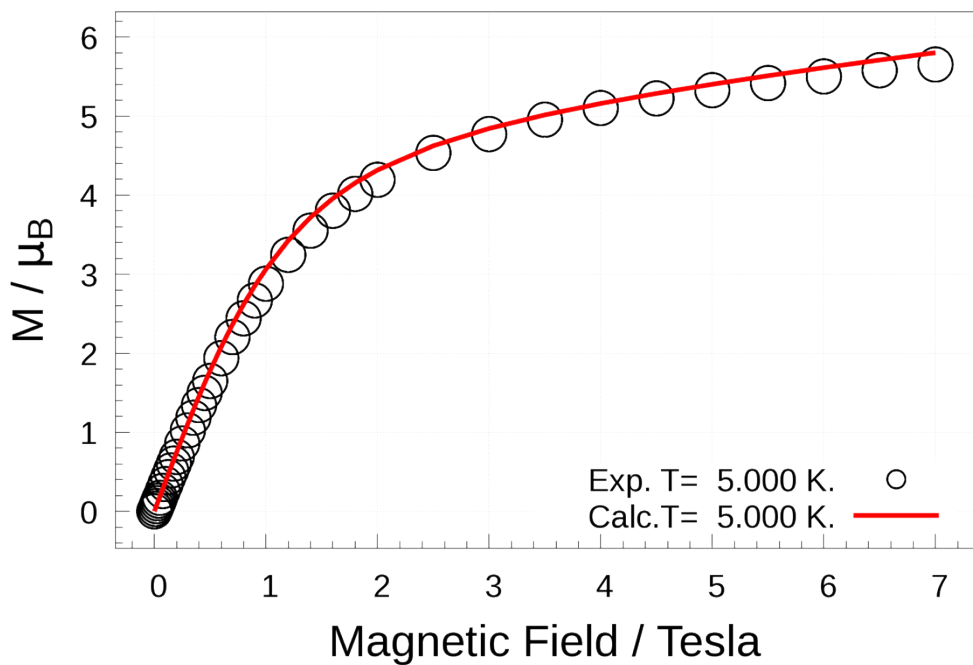


**Figure S21.** Experimental (circles) vs. calculated (red solid line) field-dependent magnetization of Dy1 at 5.0 K.

## References:

- S1 I. F. Galván, M. Vacher, A. Alavi, C. Angeli, F. Aquilante, J. Autschbach, J. J. Bao, S. I. Bokarev, N. A. Bogdanov, R. K. Carlson, L. F. Chibotaru, J. Creutzberg, N. Dattani, M. G. Delcey, S. S. Dong, A. Dreuw, L. Freitag, L. M. Frutos, L. Gagliardi, F. Gendron, A. Giussani, L. Gonzalez, G. Grell, M. Guo, C. E. Hoyer, M. Johansson, S. Keller, S. Knecht, G. Kovačević, E. Källman, G. Li Manni, M. Lundberg, Y. Ma, S. Mai, J. P. Malhado, P. Å. Malmqvist, P. Marquetand, S. A. Mewes, J. Norell, M. Olivucci, M. Oppel, Q. M. Phung, K. Pierloot, F. Plasser, M. Reiher, A. M. Sand, I. Schapiro, P. Sharma, C. J. Stein, L. K. Sørensen, D. G. Truhlar, M. Ugandi, L. Ungur, A. Valentini, S. Vancoillie, V. Veryazov, O. Weser, T. A. Wesołowski, P.-O. Widmark, S. Wouters, A. Zech, J. P. Zobel and R. Lindh, *J. Chem. Theory Comput.*, 2019, **15**, 5925–5964.
- S2 P. E. M. Siegbahn, J. Almlöf, A. Heiberg and B. O. Roos, *J. Chem. Phys.*, 1981, **74**, 2384 – 2396.
- S3 J. Olsen, B. O. Roos, P. Jørgensen and H. J. A. Jensen, *J. Chem. Phys.*, 1988, **89**, 2185 – 2192.
- S4 P. Å. Malmqvist, B. O. Roos and B. Schimmelpfennig, *Chem. Phys. Lett.*, 2002, **357**, 230– 240.
- S5 L. Ungur and L. F. Chibotaru, “SINGLE\_ANISO program,” can be found under <http://www.molcas.org/documentation/manual/>